

Stable Copper–Nitrosyl Formation by Nitrite Reductase in Either Oxidation State<sup>†</sup>Elitza I. Tocheva,<sup>‡</sup> Federico I. Rosell,<sup>§</sup> A. Grant Mauk,<sup>§</sup> and Michael E. P. Murphy<sup>\*,‡,§</sup>

Department of Microbiology and Immunology and Department of Biochemistry and Molecular Biology, Life Sciences Institute, University of British Columbia, 2350 Health Sciences Mall, Vancouver BC, V6T 1Z3, Canada

Received June 18, 2007; Revised Manuscript Received August 17, 2007

**ABSTRACT:** Nitrite reductase (NiR) is an enzyme that uses type 1 and type 2 copper sites to reduce nitrite to nitric oxide during bacterial denitrification. A copper–nitrosyl intermediate is a proposed, yet poorly characterized feature of the NiR catalytic cycle. This intermediate is formally described as Cu(I)–NO<sup>+</sup> and is proposed to be formed at the type 2 copper site after nitrite binding and electron transfer from the type 1 copper site. In this study, copper–nitrosyl complexes were formed by prolonged exposure of exogenous NO to crystals of wild-type and two variant forms of NiR from *Alcaligenes faecalis* (A/NiR), and the structures were determined to 1.8 Å or better resolution. Exposing oxidized wild-type crystals to NO results in the reverse reaction and formation of nitrite that remains bound at the active site. In a type 1 copper site mutant (H145A) that is incapable of electron transfer to the type 2 site, the reverse reaction is not observed. Instead, in both oxidized and reduced H145A crystals, NO is observed bound in a side-on manner to the type 2 copper. In A/NiR, Asp98 forms hydrogen bonds to both substrate and product bound to the type 2 Cu. In the D98N variant, NO is bound side-on but is more disordered when observed for the wild-type enzyme. The solution EPR spectra of the crystallographically characterized NiR–NO complexes indicate the presence of an oxidized type 2 copper site and thus are interpreted as resulting from stable copper–nitrosyls and formally assigned as Cu(II)–NO<sup>−</sup>. A reaction scheme in which a second NO molecule is oxidized to nitrite can account for the formation of a Cu(II)–NO<sup>−</sup> species after exposure of the oxidized H145A variant to NO gas.

Bacterial dissimilatory denitrification is a crucial component of the global nitrogen cycle (1). The enzymes that mediate denitrification are induced by low oxygen tension and are responsible for the stepwise reduction of nitrate and nitrite to dinitrogen in an anaerobic respiratory process. The committed step of the denitrification process is the reduction of nitrite to nitric oxide by the enzyme nitrite reductase (NiR<sup>1</sup>) (2). Two distinct types of nitrite reductases have been identified that catalyze the same reaction (NO<sub>2</sub><sup>−</sup> + 2H<sup>+</sup> + e<sup>−</sup> → NO + H<sub>2</sub>O) even though they share no significant sequence identity, employ two distinct mechanisms, and rely on different cofactors at the catalytic site (3).

Cytochrome *cd*<sub>1</sub> NiRs are found in the periplasmic space in two-thirds of isolated denitrifiers (4). High-resolution

crystal structures of cytochrome *cd*<sub>1</sub> NiRs from *Thiosphaera pantotropha* (5) and *Pseudomonas aeruginosa* (6) reveal that these enzymes consist of two identical, 60 kDa subunits. Each monomer contains one heme *c* prosthetic group covalently linked to the polypeptide chain and one heme *d*<sub>1</sub> group (5, 7). The well-accepted catalytic mechanism of these enzymes is initiated with nitrite binding via the nitrogen atom to the ferrous *d*<sub>1</sub> heme. Upon reduction of nitrite, a heme iron–nitrosyl intermediate is formed with NO coordinated to the iron in an end-on fashion via the nitrogen atom. The product diffuses out of the active site and an electron transfer from the *c* heme restores the enzyme in its resting state (5).

In contrast, the copper-containing enzymes, including that from *Alcaligenes faecalis* S-6 (A/NiR), are homotrimers with two spectroscopically distinct copper sites per monomer (8, 9). A type 1 copper site is situated near the protein surface where it is poised to receive electrons from biological electron donors such as pseudoazurin. This copper atom is coordinated by two histidines, a cysteine and a methionine. The second copper ion is coordinated by three histidines and a water molecule in the resting, oxidized state of the enzyme and is classified as a type 2. This copper atom is located at the interface between two adjacent monomers and is the site of nitrite reduction to nitric oxide. The two copper sites are approximately 12 Å apart, but they are coupled by a His-Cys bridge that promotes efficient electron transfer between the two copper sites.

In contrast to the *cd*<sub>1</sub> NiRs, the catalytic mechanism of Cu NiRs remains controversial owing to the paradox between the observed O-coordination of nitrite and the N-coordination

<sup>†</sup> This work was supported by an NSERC Discovery Grant (M.E.P.M.), CIHR Grant MOP-97182 (A.G.M.), a Canada Research Chair (A.G.M.), and a UBC University Graduate Fellowship (E.I.T.). Portions of this research were carried out at the Stanford Synchrotron Radiation Laboratory, a national user facility operated by Stanford University on behalf of the U.S. Department of Energy, Office of Basic Energy Sciences. The SSRL Structural Molecular Biology Program is supported by the Department of Energy, Office of Biological and Environmental Research, and by the National Institutes of Health, National Center for Research Resources, Biomedical Technology Program.

\* To whom correspondence should be addressed. Tel: 604-822-8022. Fax: 604-822-6041. E-mail: Michael.Murphy@ubc.ca.

<sup>‡</sup> Department of Microbiology and Immunology.

<sup>§</sup> Department of Biochemistry.

<sup>1</sup> Abbreviations: NiR, nitrite reductase; A/NiR, nitrite reductase from the bacterium *Alcaligenes faecalis*; EPR, electron paramagnetic resonance; ENDOR, electron-nuclear double resonance; D98N, Asp98Asn mutant of A/NiR; H145A, His145Ala mutant of A/NiR; SSRL, Stanford Synchrotron Radiation Laboratory.

of metal–nitrosyls characterized chemically. Interestingly, the crystal structure of the product-bound reduced AfNiR reveals that NO binds to the type 2 copper atom in a side-on fashion, such that both the N and the O atoms are equidistant from the metal ion (10). On the basis of EPR spectroscopy, the presumed {CuNO}<sup>11</sup> system was assigned formally as a Cu(II)–NO<sup>−</sup> complex. This unusual copper–nitrosyl structure led to a proposed catalytic mechanism for Cu NiRs assuming a copper–nitrosyl intermediate {CuNO}<sup>10</sup> with a side-on binding mode similar to that observed crystallographically (10).

Few copper–nitrosyls have been characterized to date. Recently, however, Usov et al. characterized the formation of copper–nitrosyl complexes in NiR from *Rhodobacter sphaeroides* following addition of NO gas or by generation of NO in a single turnover reaction (11). Notably, NO is described by the authors as interacting with a reduced type 2 copper atom to form a Cu(I)–NO• complex with no immediate electron transfer in the ground state between the copper and the radical. Interest in copper–nitrosyl formation has also led to the synthesis of biomimetic compounds of Cu NiRs. One of these compounds with nitrogenous copper ligands, prepared under reducing conditions and reacted with NO, was characterized by both X-ray crystallography and EPR spectroscopy (12). The crystal structure indicates end-on binding of NO to the copper via the nitrogen atom. The EPR spectrum exhibits a *g* value of 1.84 which is lower than typical values for Cu(II) (*g* > 2), so this copper–nitrosyl was not described as a Cu(II)–NO<sup>−</sup> species. However, integration of the copper signal of the complex revealed that ~70% of the available copper interacted with NO and contributed to the observed signal (12). Furthermore, DFT calculations on copper–nitrosyl model systems suggest that side-on and end-on NO coordination to copper are nearly isoenergetic (13).

In the wild-type NiR, the side-chain carboxylate of Asp98 forms hydrogen bonds to both product and substrate bound to the type 2 copper (10, 14). Mutating Asp to Asn (D98N) results in the loss of the Asp98 hydrogen bond to the oxygen atom (O2) of nitrite that coordinates to the copper. This interaction is suggested to explain the 100-fold decrease in specific activity of the D98N variant (15). A mutation of the type 1 ligand histidine to an alanine (H145A) results in an increase of the reduction potential of the site such that it remains in the reduced state (16). In this inactive variant, internal electron transfer from the reduced type 1 to the oxidized type 2 site does not occur regardless of the presence of potential exogenous type 1 ligands (16).

In this study, both the D98N and H145A variants were examined for copper–nitrosyl formation upon addition of exogenous NO. While the D98N variant was used to determine the role of Asp98 in defining the binding mode of NO, the H145A variant was used to study the interactions of the type 2 copper of NiR with NO without the possibility of electron transfer to or from the type 1 site upon formation of the copper–nitrosyl complex. Crystal structures were obtained of oxidized AfNiR exposed to NO, reduced and oxidized H145A exposed to NO, and reduced D98N exposed to NO. For each X-ray structure, complementary EPR data were collected to ascertain the oxidation states of the copper sites and to gain further insight into the electronic structure

of the copper–nitrosyls. The data are interpreted in terms of the proposed catalytic mechanism for Cu NiR.

## EXPERIMENTAL PROCEDURES

**Protein Purification and Crystallography.** Recombinant wild-type AfNiR, D98N, and H145A were expressed and purified from *Escherichia coli* as described previously (16, 17). Crystals were grown at room temperature by the hanging-drop vapor diffusion method with equal volumes (1  $\mu$ L) of reservoir and protein solutions (9, 17). The protein solutions were concentrated to 25–40 mg/mL and buffered in 20 mM Tris, pH 7.0. AfNiR crystals grew using reservoir solutions consisting of 6–11% polyethylene glycol 4000 and 0.1 M sodium acetate buffer, pH 4. Crystals of the H145A variant were grown with 6–11% polyethylene glycol 6000, 0.1 M ammonium sulfate, and 0.01 M sodium acetate buffer, pH 4.5, and crystals of the D98N variant were grown with 7–12% polyethylene glycol 4000, 75 mM acetamide, and 10 mM sodium acetate buffer, pH 4. Under these conditions, crystals grew typically to dimensions of 0.1  $\times$  0.1  $\times$  0.2 mm within 3 days.

For the preparation of all NO-soaked protein crystals, reservoir solutions and crystal suspensions were deoxygenated by exchanging with argon. NO-saturated reservoir solutions were prepared by passing NO gas (Praxair) through a NaOH column and subsequently purging the solutions at 1 atm. All materials were then transferred into an MBraun Labmaster anaerobic glovebox (Stratham, NH) in which O<sub>2</sub> levels were  $\leq$  2 ppm. The NO-saturated solutions were sealed during incubation of the samples in the glovebox. Crystals of the oxidized AfNiR and H145A were soaked in NO-saturated solutions for 20 min. Preparation of the reduced H145A and D98N crystals exposed to NO was achieved by first reducing the crystals in 20 mM ascorbate for 30 min. The crystals were then transferred to fresh reservoir solutions without ascorbate to remove excess reductant. Finally, the crystals were soaked in NO-saturated solutions for 20 min. Prior to anaerobic immersion in liquid nitrogen, all crystals were submerged in reservoir solutions supplemented to 30% glycerol as a cryoprotectant.

X-ray crystallography data were collected to resolutions of 1.8 Å or better on beam lines 11-3, 1-5, or 9-1 at SSRL. Statistics of data processing and structure refinement are presented in Table 1. The data were processed with DENZO and scaled with SCALEPACK (18). Five percent of the data were set aside to calculate the free *R*-factor (19) after conversion to structure factor amplitudes. Refinement was accomplished using the program REFMAC (20), and all model building and visualizations were carried out using the program O (21). All crystals presented are of a primitive orthorhombic lattice (*P*<sub>2</sub><sub>1</sub><sub>2</sub><sub>1</sub>) and contain the assembled trimer in the asymmetric unit. The crystals were isomorphous with the crystal of the reduced, NO-bound AfNiR (PDB code 1SNR) which was used as the starting model in refinement. For the oxidized, NO-soaked AfNiR structure, all the water molecules, exogenous ligands, and the side chain of Asp98 were removed from the starting model. In addition, the side chain of His145 was removed from the initial model prior to refinement of the H145A complex structures. In all structures, the metal–ligand interactions were unrestrained, and the N–O bond of nitric oxide was restrained to 1.45 Å.

Table 1: Data Collection and Refinement Statistics<sup>a</sup>

crystal	oxidized		reduced	
	AfNiR exposed to NO	H145A–NO	H145A–NO	D98N–NO
	Data Collection			
resolution (Å)	30–1.6 (1.66–1.6)	30–1.8 (1.86–1.8)	30–1.75 (1.81–1.75)	30–1.65 (1.71–1.65)
space group	$P2_12_12_1$	$P2_12_12_1$	$P2_12_12_1$	$P2_12_12_1$
unit cell dimensions (Å)	$a = 61.1$ $b = 101.8$ $c = 145.5$	$a = 61.0$ $b = 102.1$ $c = 145.8$	$a = 61.1$ $b = 101.9$ $c = 145.7$	$a = 61.4$ $b = 102.4$ $c = 146.1$
unique reflections	116657	84022	92217	111459
completeness (%)	95.5 (88.6)	98.6 (96.5)	99.4 (99.9)	100 (100)
average $I/\sigma I$	15.0 (3.0)	22.4 (2.8)	18.7 (3.3)	20.4 (5.5)
redundancy	3.3	3.4	4.0	7.3
$R_{\text{sym}}$ (%)	8.7 (42.2)	5.5 (52.2)	7.6 (50.5)	10.1 (52.0)
	Refinement			
$R_{\text{work}}$ (%)	16.1 (22.0)	18.8 (26.7)	17.2 (25.1)	14.9 (19.1)
$R_{\text{free}}$	18.2 (28.7)	21.2 (30.9)	19.6 (27.2)	17.0 (23.2)
coordinate error <sup>b</sup> (Å)	0.05	0.09	0.07	0.05
average $B$ -factors (Å <sup>2</sup> )	19.9	28.9	23.6	19.0
rms deviations from ideality				
bond lengths (Å)	0.009	0.010	0.010	0.010
bond angles (deg)	1.295	1.281	1.243	1.271

<sup>a</sup> Values reported in parentheses refer to the highest resolution shell. <sup>b</sup> Coordinate error derived from maximum likelihood refinement.

**EPR Spectroscopy.** Protein solutions (1.6 mM of AfNiR monomer, 0.6 mM of D98N monomer or 2.2 mM of H145A monomer) were prepared in 20 mM Tris buffer, pH 7.0 and were dialyzed overnight in an anaerobic glovebox against 50 mM MES, 50 mM acetate, pH 4 (buffer A). Reference spectra of each sample (300  $\mu$ L) were collected prior to further treatment. Protein samples were then reduced by dialysis for 2 h against buffer A supplemented with 20 mM ascorbate in the glovebox. Complete reduction of each sample was verified by EPR spectroscopy (data not shown). Excess reductant was removed by two successive, 2 h anaerobic dialysis steps against buffer A. The reduced proteins were then dialyzed for 20 min or 90 min against NO-saturated buffer A in the glovebox. Samples prepared in this manner were transferred into precision bore EPR tubes (Wilmad, NJ), sealed with an airtight rubber septum, removed from the glovebox, and submerged immediately in liquid nitrogen.

X-band EPR spectra were recorded at 80 K with a Bruker ESP300E spectrometer equipped with a Hewlett-Packard model 5352B frequency counter and quartz finger dewar. Parameters used for data collection were as follows: modulation frequency 100 kHz, modulation amplitude 1 to 10 G, microwave frequency 9.4 to 9.8 GHz, microwave power 0.5 to 10 mW.

**Spin Quantification.** Spin quantification was used to determine the amount of oxidized copper present after reduced and oxidized H145A variant protein samples were exposed to NO. The standard solution used for these experiments was a 1.00 mM CuCl<sub>2</sub> solution in 10 mM HCl and 1 M sodium perchlorate. Equal volumes of protein sample and standard were used in either case, and the readings were performed in the same high precision bore EPR tube (Wilmad, NJ). The spectra were integrated and the area underneath the curve was calculated with the program WinEPR. The proportion of oxidized metal in each sample was estimated based on the assayed copper content

of each sample by the BCA method (22) and the amount measured by EPR.

## RESULTS

The overall protein folds of the NO-treated AfNiR and the NO-treated D98N and H145A variants were essentially identical to that defined by the crystal structure of native AfNiR (PDB entry 1AS7) as reflected by an rms deviation between the C $\alpha$  atoms of less than 0.2 Å. For all the structures presented here, the major structural differences, other than those in the vicinity of mutations, are localized around the type 2 copper sites. The final refined models of the crystal structures consist of three peptide chains. Chains A and C include residues from Ala4 to Gly339, and chain B includes residues from Ala4 to Thr340. Ramachandran plots of the main chain torsional angles in each structure show that 95.0% of the residues are in the most favored regions and none is observed in the disallowed regions as defined by PROCHECK (23).

**Crystal Structures of Oxidized AfNiR and H145A Exposed to NO.** In the oxidized, NO-exposed AfNiR crystal structure, a well-defined omit electron density map in the region of the type 2 copper site revealed density in the apical position of the copper that could best be modeled as a nonlinear molecule of three atoms (Figure 1A). This density was modeled as nitrite coordinating to the type 2 copper by the O2 oxygen atom (average Cu–O2 distance 2.06 Å, Table 2). A refined average  $B$ -factor of 32 Å<sup>2</sup> indicates that the nitrite is well ordered. The nitrite is oriented almost face-on with respect to the copper ion, such that both the nitrogen (2.48 Å) and second oxygen (2.31 Å) atom are in close proximity to the metal atom. A hydrogen bond is formed between the O2 atom of nitrite and the O $\delta$ 1 atom of residue Asp98 (2.63 Å). Nitrite coordinates to the type 2 copper in each of the three monomers in the asymmetric unit. In subunits B and C, additional electron density is observed for a fourth atom. These sites are refined with both nitrite and acetate molecules coordinated to the type 2 center at

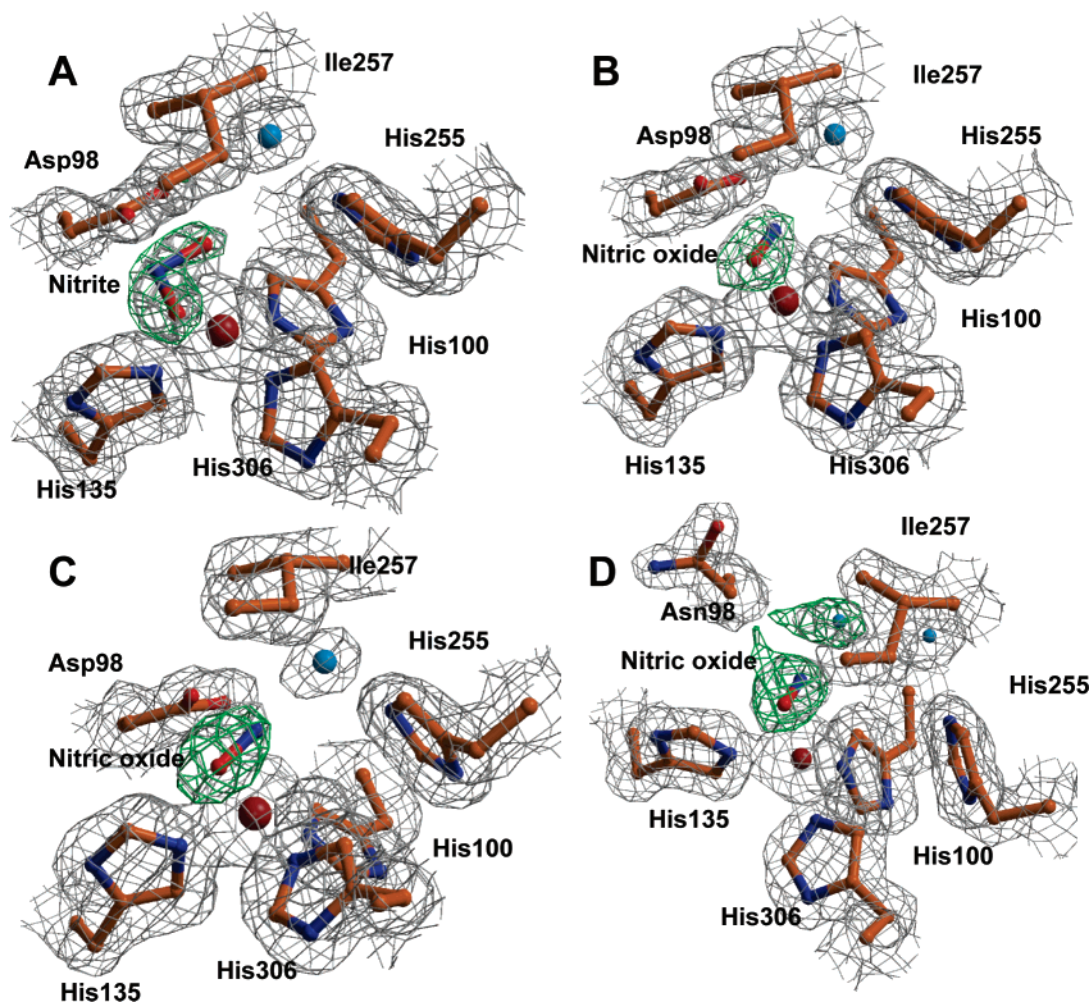


FIGURE 1: Crystal structures of wild-type and mutant forms of *AfNiR* exposed to NO: (A) oxidized, wild-type *AfNiR* with a nitrite molecule coordinating to the copper (subunit A); (B) oxidized H145A with NO bound to the copper (subunit A); (C) reduced H145A with a NO molecule bound side-on to the copper (subunit B); (D) reduced D98N exposed to NO shows disorder in the binding of NO (subunit A).  $2F_o - F_c$  (gray) and omit  $F_o - F_c$  (green) electron density maps of type 2 copper site are contoured at 1.0 and 5  $\sigma$ , respectively. In each panel, the carbon atoms are colored in orange, the nitrogen atoms are colored in blue, and the oxygen atoms are in red. The type 2 copper ion is colored in light blue, and a catalytically important water molecule is colored in light blue. Figure 1 was created with the programs Molscript (37) and Raster3D (38).

Table 2: Nitrite and NO Bond Distances ( $\text{\AA}$ )<sup>a</sup>

interatomic distance	oxidized wild-type <i>AfNiR</i> bound to $\text{NO}_2^-$ <sup>b</sup>	reduced wild-type <i>AfNiR</i> bound to NO <sup>b</sup>	oxidized wild-type <i>AfNiR</i> , exposed to NO ( $\text{NO}_2^-$ bound)	oxidized H145A–NO <sup>d</sup>	reduced H145A–NO <sup>e</sup>	reduced D98N–NO
O2–Cu	2.06 (0.02)	n/a	1.99 (0.01)	n/a	n/a	n/a
N–Cu	2.33 (0.03)	1.99 (0.02)	2.48 (0.05)	1.99 (0.04)	2.00	2.16 (0.03)
O1–Cu <sup>c</sup>	2.34 (0.05)	2.0 (0.1)	2.3 (0.1)	2.1 (0.1)	1.95	2.36 (0.06)
ligand–O $\delta$ 1Asp98	2.57 (0.05)	2.58 (0.07)	2.63 (0.07)	2.6 (0.2)	2.89	n/a

<sup>a</sup> Bond distances are averaged over all three monomers. Numbers in parentheses correspond to the deviation from the average. <sup>b</sup> From reference (10). <sup>c</sup> Ligand distances for nitrite only. <sup>d</sup> Subunits A and B. <sup>e</sup> Subunit B only.

50% occupancy each (see Supporting Information, Figure S1A and B). In addition, the proximal Asp98 is partially disordered in the B and C sites and refines in two predominant conformations at 50% occupancy each. As in subunit A, when nitrite is bound to the copper, Asp98 forms a hydrogen bond to the substrate and is pointed toward the copper. However, when acetate is bound at the active site, the side chain of the Asp98 is displaced and points away from the metal atom. The space vacated by this alternate conformation of Asp98 is filled partially by a solvent molecule. This water molecule forms two hydrogen bonds:

one to the bridging water, which in the native structure connects Asp98 and His255, and the other to the O2 atom of acetate.

In the structure of oxidized, NO-exposed H145A, extra electron density observed in the apical position could accommodate at most two atoms. In subunits A (Figure 1B) and B (see Supporting Information, Figure S1C), this density is modeled as nitric oxide coordinated side-on to the type 2 copper such that the nitrogen and the oxygen are equidistant from the copper ion. Even though it is not possible to distinguish crystallographically between the N and the O

atoms of the NO molecule, as assigned, the two NO molecules in the asymmetric unit refine to an average  $B$ -factor of  $31 \text{ \AA}^2$ , and the average ligand bond lengths are  $1.99 \text{ \AA}$  for Cu–N and  $2.09 \text{ \AA}$  for Cu–O (Table 2). The assignment of the N and O atoms was based on the possibility of hydrogen bond formation with Asp98 ( $2.63 \text{ \AA}$ ). Previous studies suggest that Asp98 is likely deprotonated (15, 24) such that a hydrogen bond can form between the protonated N atom of NO and the O $\delta$ 1 atom of Asp98. In the refinement of monomer C, a single atom is sufficient to accommodate the electron density observed at the apical position of the type 2 copper site (see Supporting Information, Figure S1D). This density is modeled as a water molecule located  $2.01 \text{ \AA}$  from the Cu(II) ion and  $3.51 \text{ \AA}$  from O $\delta$ 1 of Asp98. This water ligand is superimposable on the water bound to the active site Cu(II) ion in the crystal structure of the resting enzyme (9). The observation of a water molecule bound to subunit C is likely due to the difference in solvent accessibility in the crystal as the result of crystal packing.

**Crystal Structure of Reduced, NO-Exposed D98N and H145A.** In the reduced NO-exposed H145A structure, the NO molecule is refined at full occupancy in subunit B such that the N and O distances to the type 2 copper are  $2.00$  and  $1.95 \text{ \AA}$ , respectively (Figure 1C, Table 2). At the type 2 copper atom of subunit A, weak density connects two peaks (see Supporting Information, Figure S2A). The peaks in subunit A were refined with two water molecules at half occupancy each. The water molecules are located  $\sim 2.01$  and  $\sim 2.19 \text{ \AA}$  from the copper atom and are separated by  $\sim 2.38 \text{ \AA}$ . In subunit C, extra electron density at the type 2 copper can accommodate a single atom and was refined as a water molecule (see Supporting Information, Figure S2B). This water molecule is  $1.95 \text{ \AA}$  from the type 2 copper and  $3.54 \text{ \AA}$  from O $\delta$ 1 of Asp98.

In the structure of the reduced D98N variant, the NO molecule bound at each type 2 copper site is partially disordered. In subunits A and B, side-on coordination to the metal ion is predominant (Figure 1D; Supporting Information Figure S2C), with N–Cu and O–Cu average bond distances of  $2.16 \text{ \AA}$  and  $2.36 \text{ \AA}$ , respectively. The NO molecules are refined at full occupancy in these subunits with final  $B$ -factors less than  $30 \text{ \AA}^2$ . In subunit C, the electron density observed at the type 2 copper site is interpreted as NO bound to the metal ion in two predominant conformations, end-on and side-on (Supporting Information, Figure S2D). Reduced D98N crystals were colorless but turned partially green upon NO exposure, suggesting partial reoxidation of the type 1 copper. Disorder is also observed in the conformation of the side chain of Asn98. In the predominant conformation of this residue in all three subunits, the side chain points away from the copper.

**EPR Spectroscopy.** The EPR spectrum of oxidized AfNiR collected at pH 4 exhibits the typical hyperfine splitting of both the type 1 and type 2 copper centers of Cu NiR despite the mildly acidic pH (Figure 2B, Table 3) (21–23). The spectra of the oxidized D98N and H145A variants recorded at pH 4 (Figures 2D and 3A, respectively; Table 3) also resemble those of the corresponding Cu NiR variants from different source organisms and recorded at different temperature or pH (14, 21, 24, 25).

Anaerobic dialysis of AfNiR and variants in solutions containing 20 mM sodium ascorbate resulted in EPR spectra

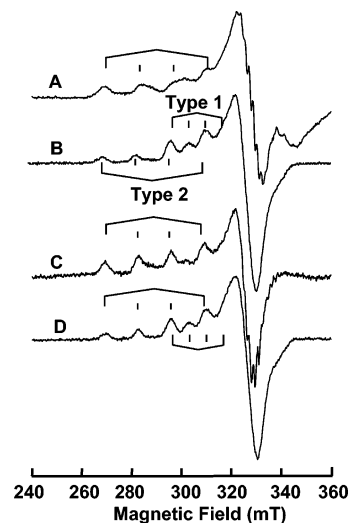


FIGURE 2: X-band EPR spectra of wild-type AfNiR and the D98N variant in 50 mM sodium acetate, 50 mM MES, pH 4: (A) reduced, NO-exposed wild-type AfNiR; (B) oxidized, wild-type AfNiR; (C) reduced, NO-exposed D98N variant; (D) oxidized D98N variant. For  $A_z$  and  $g_z$  values refer to Table 3.

Table 3: EPR Parameters for the Two Copper Sites in AfNiR<sup>a</sup>

protein sample	NO exposure time (min)	type 1		type 2	
		$A_z$	$g_z$	$A_z$	$g_z$
oxidized AfNiR	0	74	2.254	130	2.394
reduced AfNiR	20			133	2.330
oxidized D98N	0	73	2.198	129	2.331
reduced D98N	20			134	2.331
oxidized H145A	0			132	2.393
oxidized H145A	20			132	2.390
reduced H145A	20			136	2.391

<sup>a</sup> All samples are buffered in 50 mM MES, 50 mM sodium acetate pH 4.

that are devoid of any features, indicating that the proteins were fully reduced under these conditions (data not shown). Reduction of AfNiR and D98N is also evident from the disappearance of the green color associated with the oxidized type 1 copper sites for these proteins treated in this manner. Some green color of AfNiR and D98N reappeared within several minutes of exposure to NO and was stable prior to freezing the samples in liquid nitrogen. Reaction of the reduced H145A variant with NO resulted in a pale blue color. At high concentrations ( $> 1 \text{ mM}$ ), the H145A variant is a light blue color, suggesting partial oxidation of the copper site. More importantly, the EPR spectra of these samples are devoid of a type 1 copper signal. The four-line hyperfine pattern at  $g_z \sim 2.34$  with a coupling constant  $A_z \sim 134 \text{ G}$  in the EPR spectra of the three reduced proteins indicates that reaction with NO resulted in the reoxidation of the type 2 copper centers (see Figure 2A and C for AfNiR and the D98N respectively, and Figure 3C for H145A; Table 3). Binding of NO to the type 2 copper center in the three proteins gives rise to a nine-line superhyperfine pattern between 320 and 335 G ( $g_y = 2.05$ ,  $A_y = 16 \text{ G}$ ; Figure 4), indicative of binding of NO to these copper sites.

Anaerobic dialysis of the H145A variant in an NO-saturated buffer solution for 20 min without previous reduction with sodium ascorbate resulted in an EPR spectrum (Figure 3B) with the hyperfine splitting of an oxidized type

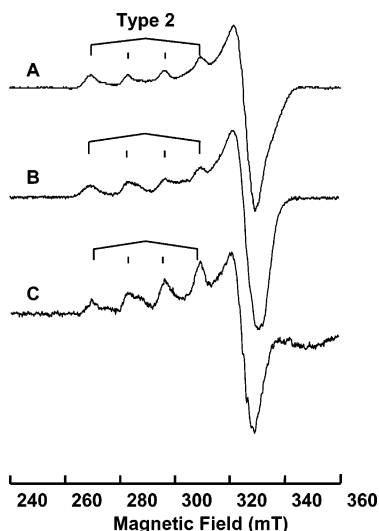


FIGURE 3: X-band EPR spectra of H145A in 50 mM sodium acetate, 50 mM MES, pH 4: (A) oxidized H145A variant; (B) oxidized, NO-exposed H145A variant; (C) reduced, NO-exposed H145A variant. For  $A_z$  and  $g_z$  values refer to Table 3.

2 copper site ( $g_z = 2.39$ ,  $A_z = 132$ ). The EPR properties of this species are similar to those identified in the spectrum of the reduced wild-type *AfNiR* exposed to NO (Table 3). Extended exposure (>90 min) of the H145A protein in either oxidation state to NO resulted in the emergence of a second, previously uncharacterized type 2 copper species ( $g_z \sim 2.35$ ,  $A_z \sim 170$  G, see Supporting Information, Figure S3B and C) which was the predominant one in solution.

## DISCUSSION

**The Reverse Reaction.** Wijma et al. characterized the pH dependence of the kinetics of *AfNiR* activity in both the forward and reverse directions (25). *AfNiR* readily catalyzes the oxidation of NO to nitrite. Exposure of the oxidized enzyme to NO in the presence of an electron acceptor yields nitrite at a rate of  $64 \text{ s}^{-1}$  at pH 7 (25). Although the forward reaction is favored below pH 7, the reverse reaction was also observed to proceed under conditions where NO and an electron acceptor are present in sufficient excess. Exposure of oxidized *AfNiR* crystals at pH 4 to a saturated NO solution produces nitrite, which remains bound to the active site copper (Figure 1A). The binding mode of nitrite and its interaction with Asp98 are the same as those observed in the structure of nitrite-soaked, oxidized *AfNiR* (10). The fate of the electron for the reverse reaction is unclear. The crystals remain green, indicating that the type 1 site either does not receive the electron or, more likely, that it quickly transfers the electron to another acceptor. Because NO is present in a substantial excess ( $\sim 1.9 \text{ mM}$  (26)), it may serve as the oxidant in a dismutation reaction to give both nitrite and  $\text{NO}^-$  (or HNO). Two molecules of HNO combine rapidly in solution to form  $\text{N}_2\text{O}$  (Scheme 1) (27, 28). Hulse and Averill proposed a catalytic mechanism in which reduction of nitrite to nitric oxide proceeds through the formation of an electrophilic nitrosyl intermediate  $\text{Cu(I)-NO}^+$  (29, 30). Similarly, upon binding of NO to an oxidized type 2 copper atom in Cu NiR, electron transfer from the radical to the metal ion also can yield an electrophilic nitrosyl intermediate ( $\text{Cu(I)-NO}^+$ ). This intermediate is susceptible to attack by nucleophiles such as water, azide, or hydroxylamine (29, 30).

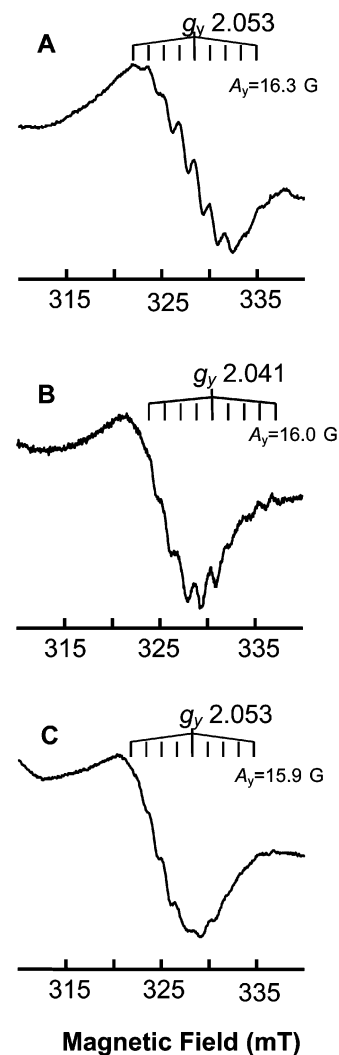
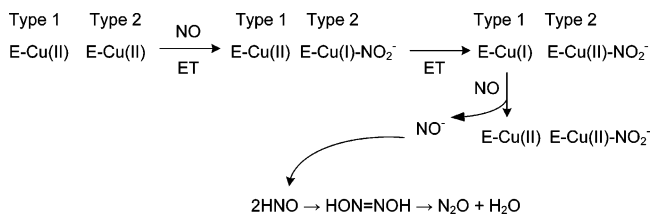


FIGURE 4: Expansion of selected spectra in Figures 2 and 3: (A) reduced wild-type *AfNiR* exposed to NO; (B) reduced, NO-exposed D98N variant; (C) reduced, NO-exposed H145A variant. In all cases a 9-line superhyperfine pattern is indicative of 4 magnetically equivalent nitrogen atoms coordinating to the type 2 copper atom. Three of these nitrogen atoms belong to histidine ligands; the fourth belongs to NO.

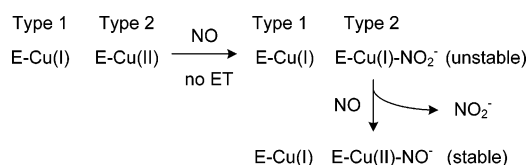
### Scheme 1



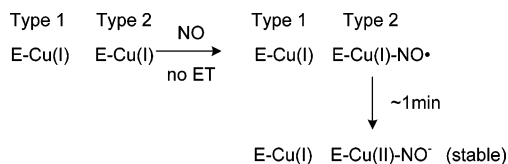
Reaction with water to give nitrite is the reverse of the dehydration step in the proposed mechanism (10).

The requirement for electron transfer to the type 1 copper in the reverse reaction is evident from the crystal structure of the oxidized H145A variant exposed to NO (Figure 1B). This variant exhibits <1% of the activity of the wild-type enzyme due to a mutation-induced increase in the reduction potential of the type 2 copper center that eliminates electron transfer to the type 1 copper center (16). Instead of producing nitrite, the addition of excess NO yields a type 2 copper that is predominantly bound by NO side-on (Figure 1B). This side-on binding mode was observed previously when reduced

## Scheme 2



## Scheme 3



wild-type *AfNiR* crystals were exposed to NO (10). Accordingly, the EPR spectrum of the oxidized H145A variant exposed to NO at the same pH reveals a type 2 copper signal (Figure 3B) similar to that observed for the reduced wild-type enzyme exposed to NO (10). This observation is particularly noteworthy since the oxidized, NO-exposed H145A variant is expected to be EPR silent (due to the coupling of the Cu(II) and NO• and the high reduction potential of the type 1 site, which remains reduced). Furthermore, NO has greater affinity for Cu(I) (12). Exposure of the reduced H145A variant to NO under similar conditions also results in side-on binding to the type 2 copper atom (Figure 1C) and a similar EPR spectrum (Figure 3C). The high similarity in both the binding mode observed in crystals and the EPR spectra in solution suggests that oxidized and reduced H145A and reduced wild-type samples yield the same stable copper–nitrosyl species proposed to be Cu(II)–NO<sup>−</sup> as illustrated in the Schemes 2 and 3.

The type 1 site in the wild-type enzyme is responsible for the intense green color of the protein; however, the H145A variant remained colorless indicating that the type 1 copper center remained reduced during X-ray data collection. Change in the oxidation state of the type 2 copper site is unlikely to be a concern since previous EXAFS analyses conducted on reduced and oxidized wild-type NiR did not show evidence of photoinduced reduction of the oxidized copper centers (31, 32).

**Stable Copper–Nitrosyl Formation.** Prolonged exposure (20 min) of the H145A variant to nitric oxide can yield the same stable copper–nitrosyl complex (Cu(II)–NO<sup>−</sup>) regardless of the starting oxidation state of the enzyme (Schemes 2 and 3). In both the crystal and solution experiments, the oxidized type 2 copper center of the H145A variant can be reduced by an equivalent of NO to yield the electrophilic nitrosyl species proposed by Hulse and Averill (29) so that, upon reaction with water, nitrite is generated. Immediately upon release of this product, another NO molecule binds to the recently reduced type 2 copper center to yield the stable nitrosyl that is also generated when starting with the fully reduced variant. Spin quantification of EPR samples prepared with the reduced and oxidized H145A protein solutions exposed to NO indicates that 60–85% of the type 2 copper atoms in the protein solution are oxidized, confirming that these are not minor but rather the predominant species in solution.

Closer inspection of the expanded  $g_y$  region in the EPR spectra of the reduced, NO-treated D98N and H145A variants

(Figure 4B and C) reveals a similar nine-line superhyperfine splitting pattern as observed in the spectrum of wild-type NiR exposed to NO at pH 4 (Figure 4A) and pH 7 (10). The nine-line superhyperfine splitting pattern is diagnostic of the coordination of the metal center by four magnetically equivalent nitrogen ligands. In all cases,  $A_y$  is  $\sim 16$  G and  $g_y$  is 2.04–2.05. In the spectrum of the D98N variant this splitting pattern appears centered at a slightly greater magnetic field that probably reflects in part the disorder in NO coordination and longer bond distances to the metal.

Crystallographic data show that the interactions of NO with the reduced and oxidized forms of H145A are structurally similar (Figure 1B and C). However, the EPR spectra of the corresponding samples reveal some differences (Figure 3B and C). The most noteworthy of these differences appears in the  $g_y$  region of the spectra where the superhyperfine splitting pattern appears to be dependent on the starting oxidation state of the protein sample. The absence of this feature in the oxidized H145A–NO spectrum (Figure 3B) could be due to the broadening of the lines such that no signal is observed, or it could stem from subtle differences in sample preparation. Furthermore, reaction of NO with the oxidized variant (Scheme 2) differs from the reaction with the reduced variant (Scheme 3) in that reaction with the oxidized protein produces nitrite. However, a 20 min dialysis of the sample would be sufficient to remove this byproduct from the reaction. Further analysis is required to identify the origin of these spectral differences.

Side-on interactions of NO with metal centers are stabilized by the donation of electron density from the  $\sigma$  orbital on NO onto the metal and by back-donation of electron density from the occupied metal d-orbitals to the  $\pi^*$  antibonding orbitals of the NO ligand (33). The copper–nitrosyl species observed in this work differ from the complexes recently characterized by EPR-ENDOR spectroscopy (11). When samples of reduced NiR were frozen within 1 min of adding exogenous NO, signals associated with the NO• radical were the principal signals detected by EPR (11). ENDOR studies on the complex were interpreted as arising from end-on coordination of NO to the metal. Exactly how a radical can interact with a metal ion without prompt electron transfer remains unclear even if the species formed are short-lived. Furthermore, the presence of additional equivalents of reductant (11) may have led to secondary electron transfer events to make definitive interpretation of the results ambiguous. In the current study, the impossibility of electron transfer from the type 1 site of the H145A variant and the removal of excess reductant limit secondary reactions to those involving NO. Under these conditions, the side-on NO interaction observed could best be described as Cu(II)–NO<sup>−</sup>.

**Role of Asp98 in Defining the Mode of NO Binding.** Of the residues in close proximity to the type 2 copper in *AfNiR*, Asp98 is the least ordered in the absence of substrate (14). Direct hydrogen bonding to the substrate (15) and product (10) results in a decrease in the  $B$ -factors of Asp98. Side-on coordination of NO to the type 2 copper is observed in the D98N crystal structure (Figure 1D); however, difference electron density maps indicate that both the NO and the side chain of Asn98 are less well ordered than those observed in the wild-type enzyme. In addition to the predominant side-on mode of binding, partial end-on coordination of the NO

to the metal is modeled in subunit C (see Supporting Information, Figure S2D). The EPR spectrum of the reduced, NO-exposed D98N complex is similar to the spectrum of the reduced wild-type AfNiR–NO complex (Figure 2C). These spectra are characterized by  $A_z$  and  $g_z$  of 130 G and 2.31, respectively, which is indicative of an oxidized type 2 copper. Taken together, the available data indicate that the hydrogen bond to Asp98 is not required for side-on binding by NO to the copper center, but it may influence the superhyperfine splitting as addressed above.

**The Mechanism of Cu NiR Catalysis.** Both Asp98 and electron transfer from the type 1 copper site are essential for nitrite reductase activity. The O $\delta$ 1 atom of Asp98 forms a hydrogen bond with both nitrite and NO bound to the type 2 copper (10, 17). An analogous hydrogen bond is not observed in the same complexes prepared with the D98N variant (15) (Figures 1D and S2D). The greatly diminished activity of this variant (15, 34) suggests that Asp98 may also interact with intermediates throughout the catalytic cycle. Characterization of variants involving substitution of ligands at the type 1 copper site has established that this site relays electrons to the catalytic center from the physiological electron donor, pseudoazurin (35, 36). For these variants, addition of chemical reductants partially restores nitrite reductase activity presumably by direct reduction of the type 2 catalytic center. Exposure of oxidized H145A variant crystals to exogenous NO did not yield the structure of the proposed catalytic intermediate (Cu(I)–NO<sup>+</sup>). Rather, the presence of excess NO resulted in a complex with one more electron (Cu(II)–NO<sup>-</sup>). In this case, exposure to NO as a substrate probably results in a single turnover that produces nitrite and reduces the type 2 copper. A second molecule of NO then binds to form a copper–nitrosyl complex that in the absence of electron transfer from the type 1 copper is kinetically stable, thereby preventing further reaction.

In one of the three monomers of the structure of the reduced H145A–NO complex, the coordination environment of the type 2 copper is modeled with two coordination positions partially occupied by water molecules. A single water molecule may occupy these two positions or two water molecules are present to form a pentacoordinate catalytic center. The positions of these water molecules suggest a potential model for NO displacement by water in the catalytic cycle. The formation of NO at the type 2 site could be followed by a transient pentacoordinate intermediate with a water molecule ultimately leading to NO release and generation of the resting state.

Presumably, the catalytic intermediate (Cu(I)–NO<sup>+</sup>) is short-lived relative to the time frame of our experiments. Within the 20 min of NO exposure of the oxidized crystals, either electron transfer to the type 1 site occurs resulting in nitrite formation in the wild-type enzyme or a second NO equivalent reduces the type 2 site in the H145A variant. Trapping the copper–nitrosyl intermediate formed during the catalytic cycle of Cu NiR may require the development of single turnover techniques in crystal.

#### NOTE ADDED IN PROOF

A paper has appeared describing in solution spectroscopic data of NO complexes with a homologous NiR from *Rhodobacter sphaeroides* (39).

#### SUPPORTING INFORMATION AVAILABLE

Additional electron density maps of ligands bound to NiR subunits not presented here. EPR spectra of reduced wild type, the H145A and D98N variants after a prolonged exposure to NO. This material is available free of charge via the Internet at <http://pubs.acs.org>.

#### REFERENCES

- Zumft, W. G. (1997) Cell biology and the molecular basis of denitrification, *Microbiol. Mol. Biol. Rev.* 61, 533–616.
- Averill, B. A. (1996) Dissimilatory nitrite and nitric oxide reductases, *Chem. Rev.* 96, 2951–2964.
- Silvestrini, M. C., Tordi, M. G., Musci, G., and Brunori, M. (1990) The reaction of *Pseudomonas* nitrite reductase and nitrite. A stopped-flow and EPR study, *J. Biol. Chem.* 265, 11783–11787.
- Coyne, M. S., Arunakumari, A., Averill, B. A., and Tiedje, J. M. (1989) Immunological identification and distribution of dissimilatory heme cd1 and nonheme copper nitrite reductases in denitrifying bacteria, *Appl. Environ. Microbiol.* 55, 2924–2931.
- Williams, P. A., Fulop, V., Garman, E. F., Saunders, N. F., Ferguson, S. J., and Hajdu, J. (1997) Haem-ligand switching during catalysis in crystals of a nitrogen-cycle enzyme, *Nature* 389, 406–412.
- Nurizzo, D., Cutruzzola, F., Arese, M., Bourgeois, D., Brunori, M., Cambillau, C., and Tegoni, M. (1998) Conformational changes occurring upon reduction and NO binding in nitrite reductase from *Pseudomonas aeruginosa*, *Biochemistry* 37, 13987–13996.
- Nurizzo, D., Silvestrini, M. C., Mathieu, M., Cutruzzola, F., Bourgeois, D., Fulop, V., Hajdu, J., Brunori, M., Tegoni, M., and Cambillau, C. (1997) N-terminal arm exchange is observed in the 2.15 Å crystal structure of oxidized nitrite reductase from *Pseudomonas aeruginosa*, *Structure* 5, 1157–1171.
- Godden, J. W., Turley, S., Teller, D. C., Adman, E. T., Liu, M. Y., Payne, W. J., and LeGall, J. (1991) The 2.3 Å X-ray structure of nitrite reductase from *Achromobacter cycloclastes*, *Science* 253, 438–442.
- Murphy, M. E. P., Turley, S., Kukimoto, M., Nishiyama, M., Horinouchi, S., Sasaki, H., Tanokura, M., and Adman, E. T. (1995) Structure of *Alcaligenes faecalis* nitrite reductase and a copper site mutant, M150E, that contains zinc, *Biochemistry* 34, 12107–12117.
- Tocheva, E., Rosell, F., Mauk, G., and Murphy, M. (2004) Side-on copper-nitrosyl coordination by nitrite reductase, *Science* 304, 876–870.
- Usov, O., Sun, Y., Grigoryants, V., Shapleigh, J., and Scholes, C. (2006) EPR-ENDOR of the Cu(I)NO complex of nitrite reductase, *J. Am. Chem. Soc.* 128, 13102–13111.
- Ruggiero, C. E., Carrier, S. M., Antholine, W. E., Whittaker, J. W., Cramer, C. J., and Tolman, W. B. (1993) Synthesis and structural and spectroscopic characterization of mononuclear copper nitrosyl complexes: models for nitric oxide adducts of copper proteins and copper-exchanged zeolites, *J. Am. Chem. Soc.* 115, 11285–11298.
- Wasbotten, I. H., and Ghosh, A. (2005) Modeling side-on NO coordination to type 2 copper in nitrite reductase: structures, energetics, and bonding, *J. Am. Chem. Soc.* 127, 15384–15385.
- Murphy, M. E., Turley, S., and Adman, E. T. (1997) Structure of nitrite bound to copper-containing nitrite reductase from *Alcaligenes faecalis*, Mechanistic implications, *J. Biol. Chem.* 272, 28455–28460.
- Boulanger, M. J., and Murphy, M. E. P. (2001) Alternate substrate binding modes to two mutant (D98N and H255N) forms of nitrite reductase from *Alcaligenes faecalis* S-6: structural model of a transient catalytic intermediate, *Biochemistry* 40, 9132–9141.
- Wijma, H. J., Boulanger, M. J., Molon, A., Fittipaldi, M., Huber, M., Murphy, M. E. P., Verbeet, M. P., and Canters, G. W. (2003) Reconstitution of the type-I active site of the H145G/A variants of nitrite reductase by ligand insertion, *Biochemistry* 42, 4075–4083.
- Boulanger, M. J., Kukimoto, M., Nishiyama, M., Horinouchi, S., and Murphy, M. E. P. (2000) Catalytic roles for two water bridged residues (Asp98 and His255) in the active site of copper-containing nitrite reductase, *J. Biol. Chem.* 275, 23957–23964.

18. Otwinowski, Z., and Minor, W. (1997) Processing of x-ray diffraction data collected in oscillation mode, *Methods Enzymol.* 276, 307–326.
19. Brunger, A. T. (1997) Free R value: Cross-validation in crystallography, *Methods Enzymol.* 277, 366–404.
20. Murshudov, G. N., Vagin, A. A., and Dodson, E. J. (1997) Refinement of macromolecular structures by the maximum-likelihood method, *Acta Crystallogr.* 53, 240–255.
21. Jones, T. A., Zou, J.-Y., Cowan, S. W., and Kjeldgaard, M. (1991) Improved methods for building protein models in electron density maps and the location of errors in these models, *Acta Crystallogr.* A47, 110–119.
22. Brenner, A. J., and Harris, E. D. (1995) A Quantitative test for copper using bicinchoninic acid, *Anal. Biochem.* 226, 80–84.
23. Laskowski, R. A., MacArthur, M. W., Moss, D. S., and Thornton, J. M. (1993) PROCHECK: a program to check the stereochemical quality of protein structures, *J. Appl. Crystallogr.* 26, 283–291.
24. Zhang, H., Boulanger, M. J., Mauk, A. G., and Murphy, M. E. P. (2000) Carbon monoxide binding to copper-containing nitrite reductase from *Alcaligenes faecalis*, *J. Phys. Chem. B* 104, 10738–10742.
25. Wijma, H., Canters, G., de Vries, S., and Verbeet, M. (2004) Bidirectional catalysis by copper-containing nitrite reductase, *Biochemistry* 43, 10467–10474.
26. Zacharia, I., and Deen, W. (2005) Diffusivity and solubility of nitric oxide in water and saline, *Ann. Biomed. Eng.* 214–222.
27. Smith, P., and Hein, G. (1960) The alleged role of nitroxyl in certain reactions of aldehydes and alkyl halides, *J. Am. Chem. Soc.* 82, 5731–5740.
28. Miranda, K., Ridnour, L., Esprey, M., Citrin, D., Thomas, D., Mancardi, D., Donzellin, S., Ink, D., Katori, T., Tocchetti, C., Ferlito, M., Paolucci, N., and Fukuto, J. (2005) Comparison of the chemical biology of NO and HNO: an inorganic perspective, *Prog. Inorg. Chem.* 54, 349–384.
29. Hulse, C. L., and Averill, B. A. (1989) Evidence for a copper-nitrosyl intermediate in denitrification by the copper-containing nitrite reductase of *Achromobacter cycloclastes*, *J. Am. Chem. Soc.* 111, 2322–2323.
30. Averill, B. A. (1994) Novel copper nitrosyl complexes: contribution to the understanding of dissimilatory, copper-containing nitrite reductases, *Agnew. Chem., Int. Ed. Engl.* 33, 2057–2058.
31. Strange, R. W., Dodd, F. E., Abraham, Z. H. L., Grossman, J. G., Brüser, T., Eady, R. R., Smith, B. E., and Hasnain, S. S. (1995) The substrate-binding site in Cu nitrite reductase and its similarity to Zn carbonic anhydrase, *Nat. Struct. Biol.* 2, 287–292.
32. Strange, R. W., Murphy, L. M., Dodd, F. E., Abraham, Z. H., Eady, R. R., Smith, B. E., and Hasnain, S. S. (1999) Structural and kinetic evidence for an ordered mechanism of copper nitrite reductase, *J. Mol. Biol.* 287, 1001–1009.
33. Richter-Addo, G., and Legzdins, P. (1992) *Metal Nitrosyls*, pp 18–19, Oxford University Press, New York.
34. Kataoka, K., Furusawa, H., Takagi, K., Yamaguchi, K., and Suzuki, S. (2000) Functional analysis of conserved aspartate and histidine residues located around the type 2 copper site of copper-containing nitrite reductase, *J. Biochem.* 127, 345–350.
35. Kukimoto, M., Nishiyama, M., Murphy, M. E. P., Turley, S., Adman, E. T., Horinouchi, S., and Beppu, T. (1994) X-ray structure and site-directed mutagenesis of a nitrite reductase from *Alcaligenes faecalis* S-6: roles of two copper atoms in nitrite reduction, *Biochemistry* 33, 5246–5252.
36. Wijma, H. J., Macpherson, I., Alexandre, M., Diederix, R. E., Canters, G. W., Murphy, M. E., and Verbeet, M. P. (2006) A rearranging ligand enables allosteric control of catalytic activity in copper-containing nitrite reductase, *J. Mol. Biol.* 358, 1081–1093.
37. Kraulis, P. (1991) MOLSCRIPT, a program to produce both detailed and schematic plots of protein structures, *J. Appl. Crystallogr.* 24, 946–950.
38. Merritt, E. A., and Bacon, D. J. (1997) Raster3D: photorealistic molecular graphics, *Methods Enzymol.* 277, 505–524.
39. Gosh, S., Dey, A., Usov, O. M., Sun, Y., Grigoryants, V. M., Scholes, C. P., and Solomon, E. I. (2007) Resolution of the spectroscopic versus crystallographic issue for NO intermediates of nitrite reductase from *Rhodobacter sphaeroides*, *J. Am. Chem. Soc.* 129, 10310–10311.

BI701205J